

LETTER TO THE EDITOR

# The kinematic of HST-1 in the jet of M87

M. Giroletti<sup>1</sup>, K. Hada<sup>2,3</sup>, G. Giovannini<sup>1,4</sup>, C. Casadio<sup>5</sup>, M. Beilicke<sup>6</sup>, A. Cesarini<sup>7</sup>, C.C. Cheung<sup>8</sup>, A. Doi<sup>9</sup>,  
H. Krawczynski<sup>6</sup>, M. Kino<sup>3</sup>, N.P. Lee<sup>10</sup>, and H. Nagai<sup>3</sup>

<sup>1</sup> INAF Istituto di Radioastronomia, 40129 Bologna, Italy e-mail: giroletti@ira.inaf.it

<sup>2</sup> The Graduate University for Advanced Studies (SOKENDAI), 2-21-1 Osawa, Mitaka, Tokyo 181-8588, Japan

<sup>3</sup> National Astronomical Observatory of Japan, 2-21-1 Osawa, Mitaka, Tokyo, 181-8588, Japan

<sup>4</sup> Dipartimento di Astronomia, via Ranzani 1, 40127 Bologna, Italy

<sup>5</sup> Instituto de Astrofísica de Andalucía, CSIC, Apartado 3004, 18080, Spain

<sup>6</sup> Department of Physics, Washington University, St. Louis, MO 63130, USA

<sup>7</sup> School of Physics, National University of Ireland, University Road, Galway, Republic of Ireland

<sup>8</sup> National Research Council Research Associate, National Academy of Sciences, Washington, DC 20001, resident at Naval Research Laboratory, Washington DC 20375, USA

<sup>9</sup> Institute of Space and Astronautical Science, JAXA, 3-1-1 Yoshinodai, Sagamihara, Kanagawa 229-8510, Japan

<sup>10</sup> Smithsonian Astrophysical Observatory, 60 Garden St., Cambridge MA 02138, USA

Received ; accepted

## ABSTRACT

**Aims.** We aim to constrain the structural variations within the HST-1 region downstream of the radio jet of M87, in general as well as in connection to the episodes of activity at very high energy (VHE).

**Methods.** We analyzed and compared 26 VLBI observations of the M87 jet, obtained between 2006 and 2011 with the Very Long Baseline Array (VLBA) at 1.7 GHz and the European VLBI Network (EVN) at 5 GHz.

**Results.** HST-1 is detected at all epochs; we model-fitted its complex structure with two or more components, the two outermost of which display a significant proper motion with a superluminal velocity around  $\sim 4c$ . The motion of a third feature that is detected upstream is more difficult to characterize. The overall position angle of HST-1 has changed during the time of our observations from  $-65^\circ$  to  $-90^\circ$ , while the structure has moved by over 80 mas downstream. Our results on the component evolution suggest that structural changes at the upstream edge of HST-1 can be related to the VHE events.

**Key words.** Radio continuum: galaxies – Galaxies: nuclei – Galaxies: jets

## 1. Introduction

The debate about the location and the mechanisms for the production of MeV/GeV, and very high energy (VHE) gamma rays in Active Galactic Nuclei (AGN) jets is very lively in the era of the *Fermi* satellite and the new generation Cherenkov telescopes (VERITAS, MAGIC, HESS). M87 is a particularly suitable laboratory for a detailed study of the properties of jets, given its proximity ( $D = 16$  Mpc), the massive black hole ( $M_{\text{BH}} \sim 6.4 \times 10^9 M_\odot$ , Gebhardt & Thomas 2009, corresponding to a scale of 1 mas  $\sim 150R_S$ ), and its conspicuous emission at all wavelengths. M87 shows a prominent radio, optical, and X-ray jet, characterized by many substructures and knots from sub-parsec to kiloparsec scale. VLBI observations of the inner jet show a well-resolved, edge-brightened structure, which starts with a wide opening angle (Junor et al. 1999; Krichbaum et al. 2005; Ly et al. 2007) and then experiences a strong collimation, with an opening angle smaller than  $10^\circ$  (Kovalev et al. 2007).

At about 0.8–0.9 arcseconds from the core, the jet suddenly re-brightens. This feature was first discussed in the optical by Biretta et al. (1999), who named it HST-1 and showed that it was moving at  $0.84c$ ; it also appeared to emit superluminal optical features with velocity  $\sim 6c$ . Superluminal components within HST-1 were later found with much finer angular resolution thanks to VLBI observations at 1.7 GHz by Cheung et al. (2007). In addition to presenting this hallmark of blazar ac-

tivity, HST-1 underwent a dramatic brightening in radio, optical, and X-rays during 2003–2006, becoming even brighter than the nucleus in X-rays (Harris et al. 2006). These facts together led Cheung et al. (2007) to propose that the flaring activity registered at VHE in 2005 (Aharonian et al. 2006) originated within HST-1. On the other hand, the VHE variability on time scales of days seemed to require a much more compact emission region, suggesting the nucleus of M87 itself as a likely site of TeV  $\gamma$ -ray production (Aharonian et al. 2006), involving, e.g., the BH magnetosphere (Neronov & Aharonian 2007) or an interaction between a fast jet spine and a slower sheath (Tavecchio & Ghisellini 2008). Indeed, a second VHE flare was observed in 2008, simultaneously to a strong increase of the 43 GHz flux density of the core, while HST-1 was in a low state (Acciari et al. 2009).

In this context, we started at the end of 2009 a program to monitor M87 at 5GHz with the European VLBI Network in real-time mode (e-EVN, Szomoru 2008) during the season of VHE observations in 2009/2010. The chosen array configuration provides a suitable combination of resolution (down to just above 1 mas), sensitivity (a few  $\times 0.1$  mJy beam<sup>-1</sup>), and field of view (several arcseconds), which permits a detailed study of the behavior of both the core and HST-1. Indeed, VHE activity was observed twice in 2010, very near in time to one of our e-EVN observations (Giroletti et al. 2010). While a detailed multifrequency study of M87 during the VHE event is presented in a ded-

icated paper (Abramowski et al. 2012), in this letter we focus on the kinematic properties of HST-1, extending the dataset of the EVN observations with archival VLBA data at 1.7 GHz, dating back to 2006. The new and archival observations are presented in Sect. 2; in Sect. 3, we describe the main results, and we discuss the implication and summarize the main conclusions in Sect. 4. Throughout the paper, we assume for M87 a distance of 16 Mpc (Tonry et al. 2001), corresponding to a scale of 1 mas = 0.078 pc; proper motion of 1 mas/yr corresponds to an apparent speed of 0.25  $c$ . The spectral index  $\alpha$  is defined such that  $S(\nu) \sim \nu^{-\alpha}$ .

## 2. Observations and data reduction

### 2.1. e-EVN data

We observed M87 with the e-EVN at 13 epochs between June 2009 and October 2011. The observing dates are given in Table 1. Typically, observations lasted 4–8 hours, and the longest baselines were achieved from European stations to Shanghai and/or Arecibo. Some observations are somewhat limited in quality, because they were obtained as targets of opportunity, or from calibration observations. These observations are noted in Table 1; overall, the data quality is adequate to warrant good signal-to-noise detections of the source structure.

For all observations, the frequency setup was centered at 5.013 GHz and divided into eight sub-bands separated by 16 MHz each for an aggregate bit rate of 1 Gbps. The data were correlated in real time at JIVE, except for the first observation, which was disk-recorded; automated data flagging and initial amplitude and phase calibration were also carried out at JIVE using dedicated pipeline scripts. The data were finally averaged in frequency within each IF, but individual IFs were kept separate to avoid bandwidth smearing. Similarly, the data were time-averaged only to 8 s to avoid time smearing.

We produced final images after several cycles of phase and amplitude self-calibration. We applied Gaussian tapers to the visibility data to maximize sensitivity to the faint and extended emission in HST-1, resulting in a beam in the range 5 – 10 mas and rms noise of 0.1 – 0.3 mJy/beam.

### 2.2. VLBA data

M87 has been observed with the VLBA at 1.7 GHz 12 times between 2006 November and 2009 August. Each of these datasets has an on-source time of  $\sim 6$  hours, with a total bandwidth of 32 MHz. We also added two observations in 2010 April, taken at 2.3 GHz, which were part of a multi-frequency VLBA experiments aimed at studying the opacity in the core of M87 (Hada et al. 2011). Each session has a total on-source time of  $\sim 15$  minutes with a total bandwidth of 32 MHz. Observing dates are summarized in Table 1.

The initial data calibration was performed in NRAO AIPS based on the standard reduction procedures. The data were averaged at short intervals (5 seconds in time and 1 MHz in frequency) to minimize smearing effects. The data of two multi-frequency experiments, which were separated by only 10 days, were combined to improve the image quality. All images were made with iterative phase and amplitude self-calibration. The resulting image rms noises in the HST-1 region are 0.1–0.3 mJy/beam. The naturally weighted images provide a typical beam size of about  $10.5 \times 5.5$  mas elongated in declination.

Overall, the final resolution and sensitivity of the VLBA and EVN data sets are well-matched. The presence of short and sen-

**Table 2.** Component motion results

Component Name	Interval (yy)	$\Delta r$ (mas)	$\beta_{\text{app}}$ ( $v/c$ )
1	2006.86-2011.80	88.1	$4.17 \pm 0.07$
2	2006.86-2011.80	81.2	$4.08 \pm 0.08$
3	2010.45-2011.80	29.8	$6.4 \pm 0.8$

sitive baselines in the EVN compensates for the spectral and resolution effects caused by the higher observing frequency.

## 3. Results

We detect significant flux density in the HST-1 region at all epochs, in addition to the bright core and the inner jet. The details of the imaging somewhat change depending on the observing frequency, the observation epoch, the  $(u, v)$ -plane coverage, and the adopted weighting scheme. In general, the flux density in the EVN images ( $\langle S_5 \rangle \sim 23$  mJy) is lower than in the VLBA ones ( $\langle S_{1.7} \rangle \sim 90$  mJy), resulting in a non simultaneous spectral index of  $\alpha = 1.2$ .

The HST-1 region extends for over 50 mas and is resolved in complex substructures. The overall position angle and the location of the individual substructures evolve with time. We model-fitted the visibility data in Difmap for all epochs, adopting elliptical Gaussian components to describe the emission from HST-1. In Fig. 1, we show ten contour images of the HST-1 region, overlaid with model-fit components. Two or three components are usually required to describe the visibility data. In Fig. 2 we plot the separation of the components from the core as a function of time. The overall uncertainty on the position at each epoch is estimated taking into account the component size and the signal-to-noise ratio. There is an additional uncertainty related to opacity effects, since the core position is not the same at the different observing frequencies. However, we estimate that any possible core-shift is significantly smaller than our estimated uncertainty on the basis of the results reported by Hada et al. (2011) and of the large overall displacement of each individual component.

Thanks to the many observations and the good accuracy in fitting the structure, we can reliably track the components between the various epochs. In particular, we are confident of the identification of the two main components, which we label as component 1 and 2, of which 1 is the outermost. The size of each component varies and additional components are present at some epochs. In particular, component 2 becomes quite extended in early 2008 and eventually splits into two components from 2008.62. After this split, the upstream subcomponent remains more or less stationary and gradually becomes fainter. When the 5 GHz observations start, there is little evidence of this component. However, starting from 2010.45, a new inner component is again required to fit the 5 GHz data. This component appears consistently thereafter and we name it component 3.

In Table 2, we summarize the displacement and velocity of each component during the campaign. Overall, components 1 and 2 have moved by very similar distances ( $\Delta r_1 = 88.1$  mas,  $\Delta r_2 = 81.2$  mas), corresponding to apparently superluminal velocities around  $\beta_{\text{app}} = 4.1$ . Thanks to the many observations, the uncertainty on this superluminal value can be constrained down to as small as a few percent. The faint substructure (identified as component 3) visible only in the last epochs at  $\sim 860 - 890$  mas from the core is also moving superluminally, but the uncertainty is larger because of the shorter time range. The identification of

**Table 1.** Log of observations.

Array	Observing Frequency	Observation date
VLBA	1.7 GHz	2006.86, 2007.08, 2007.41, 2007.63, 2007.95, 2008.09, 2008.40, 2008.62, 2008.91, 2009.14, 2009.38, 2009.64, 2010.28 <sup>a</sup>
EVN	5 GHz	2009.45 <sup>b</sup> , 2009.88, 2010.07, 2010.11, 2010.18 <sup>c</sup> , 2010.24, 2010.38, 2010.45, 2010.89, 2011.18, 2011.28, 2011.65, 2011.79

Note: <sup>a</sup> 2.3 GHz observations, averaged date for the 2010.27 and 2010.29; <sup>b</sup> calibrator observations; <sup>c</sup> ToO observation, only six stations and 128 Mbps available for self-calibration.

this component with the inner, slower feature resulting from the splitting of component 2 in 2008.62 is not straightforward.

In Fig. 3, we show the change of PA of the main emission in the HST-1 region, represented by the orientation of the vector that connects components 1 and 2. At the early epochs, HST-1 is oriented similarly to the main jet of M87 ( $\sim -65^\circ$ ). In the following epochs, the position angle progressively changes to  $-90^\circ$  and finally to  $\sim -100^\circ$  as the components move outward. In the final observations, the PA distribution presents more scatter because of the lower S/N in the data.

#### 4. Discussion

The observations presented in this letter clearly demonstrate that HST-1 is resolved in complex substructures. Two main components can be reliably identified across epochs and they are found to move with apparently superluminal velocity ( $\sim 4c$ ). From the observed speed, we can infer a range of the possible intrinsic jet velocity, assuming that the pattern and bulk velocity are the same.

The orientation angle in M87 has been widely debated in the last years. Large Doppler factors are required by the high-energy emission and the radio properties (jet brightness, superluminal motions downstream the jet, e.g. Acciari et al. 2009). Therefore, the jet has to be closely aligned with the line of sight. However, the evidence of a limb-brightened structure (Ly et al. 2007; Kovalev et al. 2007) suggests a relatively wide jet orientation angle with respect to the line of sight (Giroletti et al. 2004). Assuming a jet orientation angle in the range  $15^\circ < \theta < 25^\circ$ , the measured apparent velocity of  $4c$  corresponds to an intrinsic velocity  $0.97c < v < 0.99c$ , which in turn implies a Doppler factor and a Lorentz factor for this structure between  $\delta_{\text{HST1}} = 1.5$  and  $\Gamma_{\text{HST1}} = 6.5$  (for  $\theta = 25^\circ$ ), and  $\delta_{\text{HST1}} = 3.9$  and  $\Gamma_{\text{HST1}} = 4.1$  (for  $\theta = 15^\circ$ ), respectively. This result agrees with the synchrotron model for the X-ray emission discussed by Marshall et al. (2002) and Harris et al. (2003). By contrast, different values of the apparent velocity have been reported by other authors in other parts of the jet and/or using data obtained in different epochs (Biretta et al. 1999; Cheung et al. 2007; Kovalev et al. 2007; Ly et al. 2007; Asada et al. 2011), suggesting that the velocity structure in this jet is quite complex.

At first sight, our result does not support the identification of HST-1 as a standing-shock structure, given the displacements of  $> 80$  mas found for components 1 and 2 over  $\sim 5$  years. Moreover, no prominent stationary components were consistently detected in the 26 observations considered in this work. However, the components change in size over time, and in particular component 2 splits into substructures after 2008.62, suggesting that other features exist in HST-1 and interact with the brightest knots. Those components may be underlying, standing or very slowly moving regions, too faint to be detected separately but contributing to the total emission when brighter components are nearby. In particular, this could be the case for the D component of Cheung et al. (2007), which only becomes visi-

ble when a new feature (like our component 3) is ejected/created within HST-1. The emergence of the new superluminal component 3, upstream of 1 and 2, accompanied by a brightness decrease of 1 and 2, could eventually shift back the centroid of the arcsecond scale emission of HST-1, which would then appear to be more stationary than individual substructures. This behavior would then support the scenario in which HST-1 is a stationary reconfinement shock structure, possibly associated to a jet interaction with a gaseous condensation of the hot interstellar medium (Stawarz et al. 2006).

Based on the short variability time scales of the VHE events and on the recurrent simultaneous X-rays brightening of the core, the viability of HST-1 as the site of emission of VHE radiation has recently been severely questioned (Abramowski et al. 2012). We show the epochs of the two latest VHE flares from M87 with dotted lines in Fig. 2. Both events are followed by structural changes and rebrightening of the upstream edge of HST-1, suggesting that the origin of the VHE activity could indeed be related to the HST-1 region. A similar connection was also put forward for the 2005 VHE event: by considering a subset of the present dataset and archival VLA observations, Giovannini et al. (2011) noted a change in the proper motion velocity in HST-1 at the epoch  $\sim 2005.5$ , coincident with the TeV  $\gamma$ -ray activity and the maximum radio and X-ray flux density of the feature.

Lastly, we can discuss the properties of the magnetic field parallel to the shock front in HST-1, based on the field strength in the unshocked jet and the magnetic flux conservation. By fitting a single-zone synchrotron self-Compton model, Abdo et al. (2009) estimated a magnetic field strength at the core  $B_{\text{core}} \sim 0.055$  G. The field strength in the unshocked jet upstream of HST-1 can be estimated as  $B_{\text{jet}} = (r_{\text{HST1}}/r_{\text{core}})^{-1} B_{\text{core}} \approx 0.33 \times 10^{-3} (B_{\text{core}}/0.1 \text{ G}) \text{ G}$ , where we assume  $Br = \text{const}$  and the jet radius in HST-1 as  $r_{\text{jet}} \approx r_{\text{HST1}} \approx 15 \text{ mas} \approx 4 \times 10^{18} \text{ cm}$ , based on the images in Fig. 1. Next, let us assume that the shock dissipation occurs at HST-1. Then we can estimate the field strength downstream of the unshocked jet by the shock jump conditions. A typical strength of the compressed magnetic field at HST-1 ( $B_{\text{HST1}}$ ) can be estimated by  $B_{\text{HST1}} \approx \Gamma_{\text{jet}} B_{\text{jet}} \approx 2.3(\Gamma_{\text{jet}}/7)(B_{\text{core}}/0.1 \text{ G}) \text{ mG}$ , where  $\Gamma_{\text{jet}}$  is the bulk Lorentz factor of the unshocked jet at the HST-1-upstream, which satisfies  $\Gamma_{\text{jet}} > \Gamma_{\text{HST1}}$ . Although roughly comparable to the independently estimated value of  $B_{\text{HST1}} \delta_{\text{HST1}}^{1/3} = 1.1 \text{ mG}$  by using synchrotron cooling time at X-ray band (Harris et al. 2003, 2009), the  $B_{\text{HST1}}$  estimated here tends to be higher by a factor of several; clarifying the reasons of the discrepancy remain to be worked out.

Additional discussions on the magnetic field structure, as well as the light curve and trajectories of the individual component will therefore be treated in upcoming publications, also in the light of new planned VLBI observations. Indeed, our original aim was to address two main questions: (1) Where are the high energy gamma-rays produced in M87: the core or HST-1? (2) Is HST-1 stationary or moving? The answer to both questions may not be too simple!

*Acknowledgements.* We thank D.E.Harris for reading the manuscript. We acknowledge a contribution from the Italian Foreign Affair Minister under the bilateral scientific collaboration between Italy and Japan. e-VLBI research infrastructure in Europe is supported by the European Union's Seventh Framework Programme (FP7/2007-2013) under grant agreement no. RI-261525 NEXPRoS. The European VLBI Network is a joint facility of European, Chinese, South African and other radio astronomy institutes funded by their national research councils. The National Radio Astronomy Observatory is a facility of the National Science Foundation operated under cooperative agreement by AUI.

## References

- Abdo, A. A., Ackermann, M., Ajello, M., et al. 2009, *ApJ*, 707, 55  
Abramowski, A., Acero, F., Aharonian, F., et al. 2012, *ApJ* in press, arXiv:1111.5341  
Acciari, V. A., Aliu, E., Arlen, T., et al. 2009, *Sci*, 325, 444  
Aharonian, F., Akhperjanian, A. G., Bazer-Bachi, A. R., et al. 2006, *Sci*, 314, 1424  
Asada, K., Nakamura, M., Doi, A., et al. 2011, *IAUS*, 275, 198  
Biretta, J. A., Sparks, W. B., & Macchetto, F. 1999, *ApJ*, 520, 621  
Cheung, C. C., Harris, D. E., & Stawarz, L. 2007, *ApJ*, 663, L65  
Gebhardt, K., & Thomas, J. 2009, *ApJ*, 700, 1690  
Giovannini, G., Casadio, C., Giroletti, M., et al. 2011, *IAUS*, 275, 150  
Giroletti, M., Giovannini, G., Beilicke, M., et al. 2010, *ATel*, 2437, 1  
Giroletti, M., Giovannini, G., Feretti, L., et al. 2004, *ApJ*, 600, 127  
Hada, K., Doi, A., Kino, M., et al. 2011, *Natur*, 477, 185  
Harris, D. E., Biretta, J. A., Junor, W., et al. 2003, *ApJ*, 586, L41  
Harris, D. E., Cheung, C. C., Biretta, J. A., et al. 2006, *ApJ*, 640, 211  
Harris, D. E., Cheung, C. C., Stawarz, L., et al. 2009, *ApJ*, 699, 305  
Junor, W., Biretta, J. A., & Livio, M. 1999, *Natur*, 401, 891  
Kovalev, Y. Y., Lister, M. L., Homan, D. C., & Kellermann, K. I. 2007, *ApJ*, 668, L27  
Krichbaum, T. P., Zensus, J. A., & Witzel, A. 2005, *AN*, 326, 548  
Ly, C., Walker, R. C., & Junor, W. 2007, *ApJ*, 660, 200  
Marshall, H. L., Miller, B. P., Davis, D. S., et al. 2002, *ApJ*, 564, 683  
Neronov, A., & Aharonian, F. A. 2007, *ApJ*, 671, 85  
Stawarz, L., Aharonian, F., Kataoka, J., et al. 2006, *MNRAS*, 370, 981  
Szomoru, A. 2008, *Proceedings of Science, PoS(IX EVN Symposium)040*  
Tavecchio, F., & Ghisellini, G. 2008, *MNRAS*, 385, L98  
Tonry, J. L., Dressler, A., Blakeslee, J. P., et al. 2001, *ApJ*, 546, 681

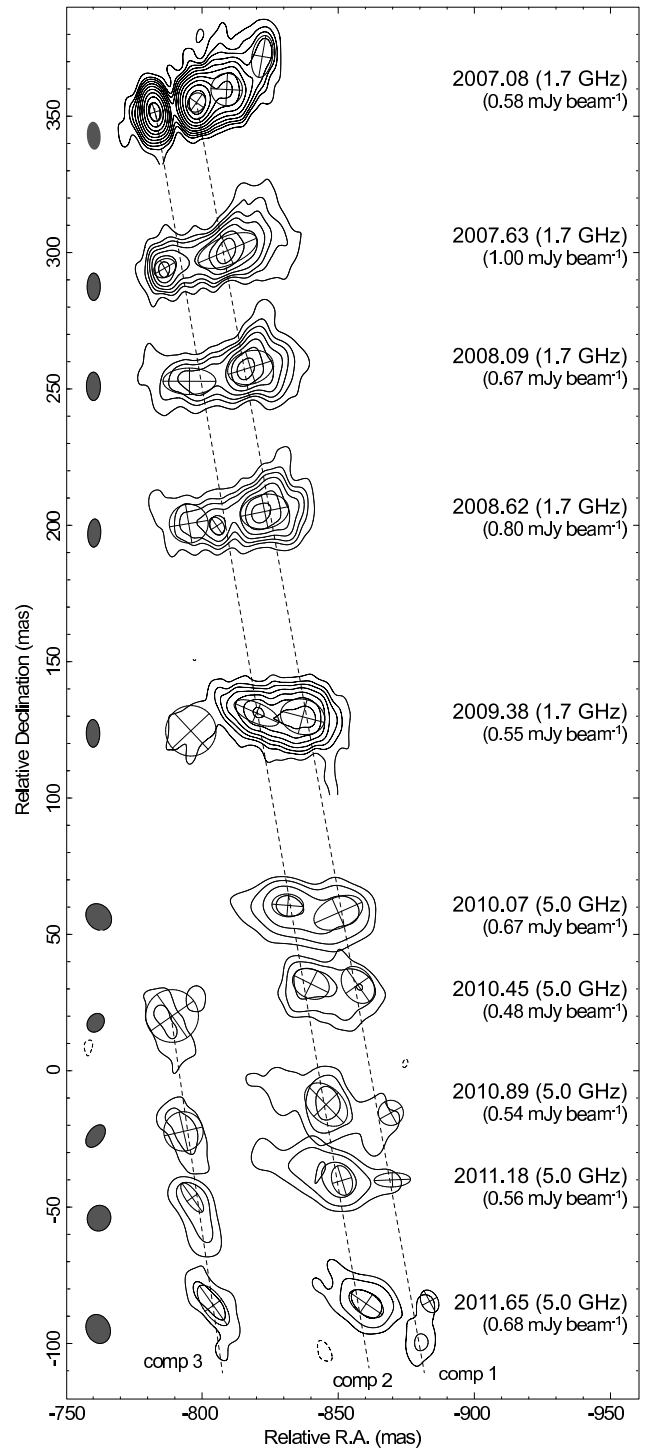


**Fig. 1.** Set of HST-1 images. For each epoch, we give the epoch, frequency, lowest contour to the right, and the restoring beam to the left of the respective contour plot. Contours are traced at  $(-1, 1, 2, 4, \dots)$  multiples of the given value. The model-fit components are overlaid as ellipses with crosses. The contour plots are spaced vertically proportionally to the time interval between the relative epochs. The axes represent the relative (RA, Dec) coordinates from the core for the first image.

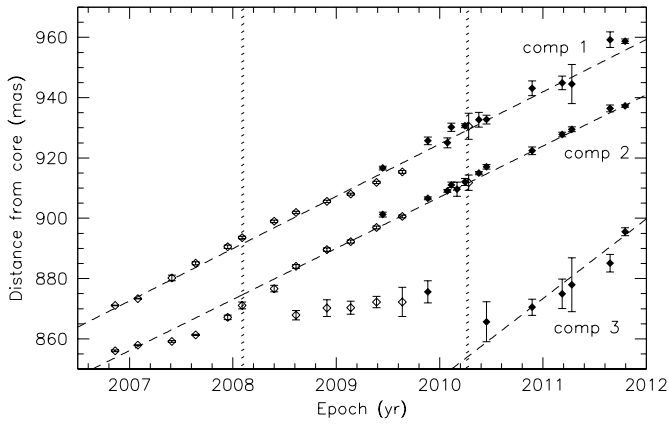


**Fig. 2.** Distance of the HST-1 sub-components from the core versus time. Empty and filled symbols show 1.7 (VLBA) and 5 GHz (EVN) data, respectively. The dashed lines show least-squares linear fits, while the vertical stripes represent the epochs of the 2008 and 2010 VHE flares.

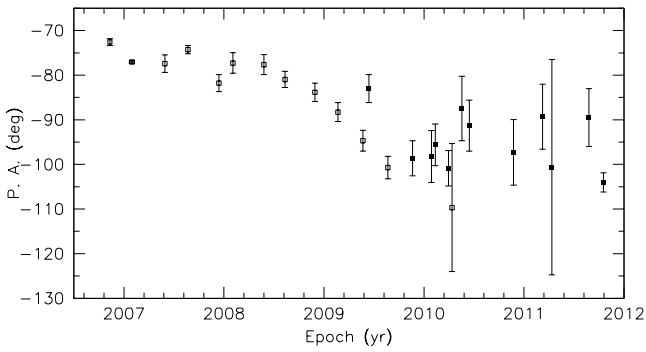


**Fig. 3.** Orientation of the vector connecting the two main components in HST-1 as a function of time.